

Lawrence Berkeley National Laboratory

Recent Work

Title

AM OPTICAL STUDY OF CATHODIC HYDROGEN EVOLUTION IN HIGH RATE ELECTROLYSIS

Permalink

<https://escholarship.org/uc/item/5vd4r308>

Authors

Landolt, Dieter

Acosta, Raul

Muller, Rolf H.

et al.

Publication Date

1969-12-01

Submitted to the Journal of the
Electrochemical Society

UCRL-19064
Preprint

c. 2

RECEIVED
LAWRENCE
RADIATION LABORATORY

FEB 19 1970

LIBRARY AND
DOCUMENTS SECTION

AN OPTICAL STUDY OF CATHODIC HYDROGEN EVOLUTION
IN HIGH RATE ELECTROLYSIS

Dieter Landolt, Raul Acosta, Rolf H. Muller and Charles W. Tobias

December 1969

AEC Contract No. W-7405-eng-48

TWO-WEEK LOAN COPY

This is a Library Circulating Copy
which may be borrowed for two weeks.
For a personal retention copy, call
Tech. Info. Division, Ext. 5545

LAWRENCE RADIATION LABORATORY
UNIVERSITY of CALIFORNIA BERKELEY

UCRL-19064

Handwritten signature

DISCLAIMER

This document was prepared as an account of work sponsored by the United States Government. While this document is believed to contain correct information, neither the United States Government nor any agency thereof, nor the Regents of the University of California, nor any of their employees, makes any warranty, express or implied, or assumes any legal responsibility for the accuracy, completeness, or usefulness of any information, apparatus, product, or process disclosed, or represents that its use would not infringe privately owned rights. Reference herein to any specific commercial product, process, or service by its trade name, trademark, manufacturer, or otherwise, does not necessarily constitute or imply its endorsement, recommendation, or favoring by the United States Government or any agency thereof, or the Regents of the University of California. The views and opinions of authors expressed herein do not necessarily state or reflect those of the United States Government or any agency thereof or the Regents of the University of California.

AN OPTICAL STUDY OF CATHODIC HYDROGEN EVOLUTION
IN HIGH RATE ELECTROLYSIS

Dieter Landolt,⁺ Raul Acosta, Rolf H. Muller and Charles W. Tobias

Inorganic Materials Research Division, Lawrence Radiation Laboratory and
Department of Chemical Engineering, University of California
Berkeley, California 94720

ABSTRACT

Hydrogen bubbles evolved cathodically under conditions encountered in electrochemical machining have been studied by stop-motion photography. Constant current densities up to 150 A/cm^2 and flow rates up to 2500 cm/sec have been employed with an experimental flow channel of 0.5 mm gap width. The observed bubble size decreased strongly with increasing flow rate and increased with increasing current density. At flow rates above 800 cm/sec , the bubble size was always below 20μ , the smallest diameter resolved by the optical arrangement used. Less gas was evolved in nitrate than in chloride electrolytes under otherwise identical conditions. The hydrogen bubbles were usually confined to a region near the cathode. Voltage oscillations and electric breakdown coincided with the appearance of a new type of bubble.

⁺Present Address: University of California
Department of Engineering
Los Angeles, California 90024

INTRODUCTION

In electrochemical machining, metals are dissolved anodically at current densities in the order of 100 A/cm^2 or higher. Hydrogen gas is formed cathodically and must be transported away from the reaction zone by the electrolyte stream. This hydrogen may affect the electrolytic process in several ways: It may increase the ohmic resistance of the electrolyte, resulting in higher cell voltage and different local current distribution. It may be oxidized at the anode and thus, decrease the current efficiency of the metal dissolution process. It may form a continuous gas blanket at the cathode and thus, lead to sparking. It may accumulate in large bubbles, which extend over the entire inter-electrode gap, and thus, drastically affect mass transfer conditions at the anode. In order to obtain a better understanding of the relative importance of such phenomena, a photographic study of cathodically generated gas bubbles was initiated. During the course of this pursuit, somewhat related work has appeared in the literature.^{1,2} In the present investigation, a more sophisticated optical arrangement has been employed and a better control and wider range of critical variables, such as current density and flow velocity have been employed in addition to the use of a well-defined flow system.

EXPERIMENTAL TECHNIQUE

The apparatus used has been described before.³ It consisted of a rectangular flow channel cell of 8 mm width and 0.5 mm height. Its sidewalls were made of flat glass plates, which provided for the optical observation of the inter-electrode gap. The total channel length was 8.5 cm, the center of the electrodes was positioned 1 cm from the downstream end. The design of the flow cell provided for fully developed

velocity profiles at the electrodes. Flow rates up to 2500 cm/sec were employed, corresponding to inlet pressures in the order of 10 atm. Since most of the pressure drop occurs in the entrance length of the flow channel, the absolute pressure at the electrodes, even at the highest flow rate employed, was only about 2 atm. Although, under these conditions, the effect of pressure on the gas volume has to be taken into account, at flow rates up to 1000 cm/sec, where most observations were made, the absolute pressure at the electrodes was only 1 to 1.3 atm, and its effect on bubble size was negligible within the accuracy of the present measurements. The copper electrodes were 3.17 mm long in the flow direction and 0.53 mm wide. Before experiments, the electrode surfaces were mechanically polished with 1 μ diamond paste, cleaned with aqueous detergent and acetone and degreased by hydrogen evolution in aqueous caustic.

The optical arrangement is shown schematically in Fig. 1*: A commercial flash light source (A) of 0.5 μ sec flash duration** was used for illumination of the gas bubbles generated in the flow cell (B) in transmitted light mode. A camera (H) with open shutter and high speed film*** was attached to a microscope tube containing a 2x objective (C) ($f = 48$ mm, N.A. = 0.08) and a 10x eyepiece (E). A small circular

* Design considerations of the optical system will be discussed elsewhere in more detail.

** EG & G 594 microflash

*** Kodak SO 340

aperture (D) of 1.6 mm diameter, located in the rear focal plane of the objective (C) served as a telecentric stop.⁴ The purpose of this device is to avoid variations in the apparent size of bubbles due to differing distances from the objective and to increase the depth of field. Unfortunately, the telecentric stop also reduces the speed and resolution of the objective, the latter being about 20 μ . In order to obtain a photographic distinction between the electrode surface and an adjacent, dense layer of gas bubbles, a pre-exposure in the absence of bubbles was made at reduced light intensity. In a typical experimental run, constant current was applied to the cell for a short period of time by switching the output of a constant current supply* from a dummy circuit to the cell circuit. A mercury relay, actuated by a pulse generator, was used for the switching. The circuit also served to trigger the flash light source after a pre-set time, which was chosen to correspond to the passage of 12 coulomb/cm². The current was switched back to the dummy load automatically after the total passage of 15 coulomb/cm². The charge passed between the start of an experiment and the moment the picture was taken, resulted in the evolution of about 1.5 cm³ hydrogen (1 atm, 298°K) per cm² electrode. This was considered sufficient to establish steady state conditions with respect to gas evolution. During the experiments, current and potentials were recorded by means of a light beam oscillograph.

* Electronic measurements C-618

EXPERIMENTAL RESULTS

Bubble Size

Typical photographs obtained in 2 N KCl solution at different flow rates and current densities are given in Figs. 2 to 4. Figure 2 illustrates the influence of flow rate and cathode orientation on bubble size for a current density of 50 A/cm^2 . An estimate of the size distribution of the bubbles for the same experiments is given in Fig. 5. These distributions were obtained by measuring the diameter of all the bubbles which were individually discernible in the whole inter-electrode gap, and determining the fraction in each size bracket of 25 microns width. The quantitative validity of the distributions given in Fig. 5 is limited for several reasons: (1) The number of measured gas bubbles (27-60) represent only part of the total gas volume and the differentiation between discernible and not discernible bubbles is subject to personal interpretation. (2) The variability of results in successive experiments probably requires a more sophisticated statistical evaluation. (3) Bubbles close to the cathode surface were usually not individually discernible and could, therefore, not be included in the count. (4) Bubbles smaller than 20μ in diameter were below the optical resolution. Qualitatively, however, Fig. 5 illustrates not only the order of magnitude of cathodically generated bubbles, but it also shows the decrease in size with increasing flow rates: the median bubble diameters are 99, 69, and 35μ for flow rates of 100, 200 and 400 cm/sec, respectively. It should also be noted that at the lower flow rates (below 400 cm/sec), a few large bubbles often existed in addition to a large number of smaller ones. It was observed during the experiments that these large bubbles were sticking to the cathode surface for prolonged periods of time while the smaller bubbles detached from areas in between. Figure 5 also

shows that the orientation of the cathode, i.e. whether it is facing up or down, has no systematic effect on size distribution, except at the lowest flow rate.

Figure 3 illustrates gas evolution at high flow rates. The size of the generated bubbles decreases rapidly with increasing velocity in this range and the size distribution becomes narrower, so that the previously observed co-existence of few large bubbles with smaller ones disappears. At flow rates of 800 cm/sec or higher, all individual bubbles were too small (below 20μ) to be resolved photographically.

The effect of current density on bubble size is illustrated in Figs. 4 and 6. A clear increase in bubble size is observed with increasing current density under otherwise identical conditions: the median bubble diameters are 56, 78 and 99μ for current densities of 5, 20 and 50 A/cm^2 , respectively. These observations are in marked contrast to findings reported by Venczel,⁵ who studied gas evolution at vertical electrodes in stagnant solutions and reported a decrease in bubble size with increasing current density. The discrepancy might possibly be explained by the different modes of convection. A bubble may be assumed to detach from the surface when external forces, such as gravity or friction with the moving liquid, become larger than the normal component of the surface tension. Since in a stagnant solution, the rate of stirring is increased when more gas is generated, higher current densities may lead to an earlier detachment of gas bubbles. In our experiments, on the other hand, local stirring was mainly due to the hydrodynamic flow and was, therefore, almost independent of current density. A decrease, rather than an increase, in bubble size with increasing current density would also be expected from the work of Kabanov and Frumkin.⁶ They showed that the contact angle, which

determines the normal component of surface tension, depends on electrode potential. For very slow hydrogen evolution on mercury, smaller contact angles and, hence, smaller bubbles were observed at increasingly negative potentials.

Force balances have been applied to the prediction of bubble size in forced convection boiling.⁷ Such a force balance for an individual bubble may be formulated as

$$F_{\sigma} = F_i + F_b \quad (1)$$

where F_{σ} is the surface tension force which holds the bubble on the electrode, F_i is the inertia force of the electrolyte acting on the bubble and F_b is the buoyancy force of the bubble. The latter can be neglected at high flow velocities. According to Tong⁷ a model of this kind predicts a decrease in bubble size with the square of the flow velocity. Such a dependence is at least qualitatively consistent with the present results. Relation (1) does, however, not account for the influence of current density and the wide distribution of bubble diameters observed at low flow rates. This distribution is at least partly due to the fact that the presence of other bubbles on the surface leads to locally varying flow conditions. Considering the fact that not even the dynamics of a single bubble, growing in a laminar velocity field, has been analyzed, no attempt has been made here to give a more detailed account of the vastly more complex case of multiple bubble dynamics in turbulent flow. Additional experimental studies should include the time-dependence of bubble growth for a more detailed description of gas evolution under the present conditions in turbulent flow. Glas and Westwater⁸ have investigated electrochemical gas evolution in stagnant solutions by high speed cinematography. They found two growth stages; an early rapid growth period, associated with bubble diameters of up to

about 50 μ , followed by a slow period. Theoretical aspects of growth mechanisms have been discussed by Cheh,⁹ who applied mass transfer considerations to predict growth rates in the slow (asymptotic) growth period. No theoretical models exist at present which predict growth rate in the rapid growth period. Since, in our study, the bubble size was often smaller than 50 μ , growth rate and residence time on the cathode surface could not be estimated on theoretical grounds.

Thickness of Two Phase Region

Figs. 2 to 4 illustrate the observation that the gas bubbles are not dispersed uniformly throughout the gap, but usually occupy a region near the cathode. At flow rates above 100 cm/sec, the thickness of this two-phase region is the same whether the cathode faces up or down. This behavior is to be expected, since at higher flow rates a gas bubble, unless it is very large, is swept away from the inter-electrode gap too fast to be affected by buoyancy. From Stoke's law, which may be applied to bubbles of less than 1 mm diameter,¹⁰ the steady state velocity due to buoyancy can be described by eq. (2).

$$v = \frac{g \rho d^2}{18\eta} \quad (2)$$

where g = gravitational constant, ρ = difference in density of gas and liquid, d = bubble diameter, η = viscosity of liquid. Assuming an electrolyte flow velocity of 400 cm/sec and a bubble diameter of 50 μ , the vertical distance traveled by the bubble due to gravity during the time needed to pass over a 3 mm long electrode is only 1.2 μ .

In order to account for the observed thickness of the two-phase region, unusually high velocities perpendicular to the flow direction are required. In Fig. 3c for example (100 A/cm², 1000 cm/sec), bubbles are found up to a distance of approximately 0.3 mm from the cathode surface. A bubble moving steadily outward from the leading edge of the electrode would need an average velocity perpendicular to the cathode of 100 cm/sec to reach this position at the downstream end of the electrode. This motion away from the cathode surface is aided by the turbulence in the liquid. Such an effect is suggested by the irregular shape of the two-phase region, which can show large variations in local thickness (Fig. 3). It is interesting to note, however, that the average thickness seems to increase little downstream from the middle of the cathode. If turbulent mixing were the only mechanism determining the spreading of the two-phase region, we would rather expect a steady increase of its average thickness in the flow direction. It is, therefore, possible that other mechanisms contribute to the dispersion of gas bubbles. An example is the "rapid fire mechanism" mentioned by Glas and Westwater,⁸ who observed that in stagnant solution, bubbles were frequently ejected from the electrode at a high velocity. This phenomenon is, at present, not well understood. The relatively smaller increase of the two-phase region in the downstream part might also be ascribed to a lower current density in this region, caused by the higher gas fraction and the associated higher ohmic resistance in the electrolyte. Dissolution of gas in the electrolyte furnishes another possible explanation for the same phenomenon. Indeed, a simple estimation shows that, under most conditions, all the gas generated could be dissolved in

the total electrolyte volume passing through the gap. For example, assuming a current density of 100 A/cm^2 , 8×10^{-6} moles of hydrogen are produced per second in our cell, while, at a flow rate of 1000 cm/sec , 40 cm^3 of electrolyte are flowing through it. A homogeneous dissolution of all the generated hydrogen would result in a concentration of 2×10^{-4} mole/liter, which is of the same order as the saturation concentration of hydrogen in potassium chloride solutions.¹¹ However, the direct dissolution of all cathodically generated gas without the formation of bubbles is, in general, not possible because the concentration gradients available under typical flow conditions are too small to account for the transport of dissolved hydrogen by convective diffusion. This is the case even under the assumption of a 1000 fold supersaturation at the electrode surface.

A rapid dissolution of initially formed gas bubbles could provide an alternate route to a homogeneous solution. This process would also affect the measured gas bubble diameters. Such a re-dissolution of gas bubbles would be similar to the behavior of vapor bubbles generated in a supercooled liquid under forced convection. Gunther¹² has shown that such bubbles became smaller and eventually disappeared upon moving downstream. The time required to dissolve 50% of the volume of a bubble of 50μ diameter can be estimated as follows: If we assume saturation concentration of the gas at the gas-liquid interface under constant pressure, and zero gas concentration in the bulk solution, the concentration difference driving force will be given by the saturation concentration, say 5×10^{-4} mole/liter. For a constant mass flux per unit area of a spherical bubble, the decrease in volume may then be expressed by eq. (3)

$$\frac{dV}{dt} = - A k C_{\text{sat}} V^{2/3} \quad (3)$$

with $A = \frac{RT}{P} 4\pi \left(\frac{3}{4\pi}\right)^{2/3}$, C_{sat} = saturation concentration, k = mass transfer coefficient (cm/sec), V = bubble volume. Integration leads to eq. (4)

$$3(V^{1/3} - V_0^{1/3}) = A k C_{\text{sat}} t \quad (4)$$

where V_0 = initial bubble volume. The time $t_{1/2}$ in which the volume is reduced to $1/2 V_0$ is

$$t_{1/2} = \frac{2.38 V_0^{1/3}}{A k C_{\text{sat}}} \quad (5)$$

With an arbitrarily assumed mass transfer coefficient of 10^{-1} cm/sec* one obtains $t_{1/2} \approx 1$ sec for 1 atm, 298°K. This time is almost four orders of magnitude larger than the residence time of a bubble moving at 1000 cm/sec between the electrodes (3×10^{-4} sec). The redissolution of gas is, therefore, too slow to produce a homogeneous gas solution between the electrodes or even to measurably affect the diameter of bubbles in our photographs.

* Since the relative motion between bubble and solution is not known, the mass transfer coefficient k has to be assumed arbitrarily. The value chosen is a maximum guess. It corresponds to the figure estimated for the electrode-solution interface at the highest flow rates employed.³

Influence of Electrolyte

Fig. 7 illustrates the surprising observation that less gas was produced at the cathode in KNO_3 than in KCl solutions, under otherwise identical conditions. The relative volume of the two-phase region in the interelectrode gap, shown in Fig. 8, has been obtained by planimetry of the areas occupied by the dispersed gas in the photographs. Since the solubility of hydrogen is about the same in both electrolytes,¹¹ the observed difference must be due to other than differences in solubility. For example, the same amount of hydrogen could appear to be smaller in nitrate solutions due to a more finely dispersed form. A more likely explanation is that, due to the reduction of nitrate at the cathode, only part of the current is used for hydrogen evolution. In the present flow apparatus, the total amount of evolved hydrogen could not be determined, but some experiments were performed in stagnant solutions of KNO_3 and KCl at 5 A/cm^2 . They confirmed that a much smaller volume of hydrogen was produced in nitrate than in chloride solution. A more quantitative investigation of cathodic reactions in nitrate solutions has been initiated. The effect of different electrolytes on the amount of cathodically formed gas was further investigated by use of chlorate and sulfate solutions. Both, photographs taken in the flow system and volumetric measurements in stagnant solutions, indicated that, within the experimental accuracy, the same amount of gas was generated in these electrolytes as in the chloride solution.

Potential measurements under high current density conditions are dominated by large ohmic drops in the electrolyte between the working electrode and the tip of the reference electrode capillary.³ The apparent cathode potentials, thus determined at constant current density,

provide an indirect measure of electrolyte conductivity and, consequently, gas volume fraction. Apparent cathode potential measurements are given in Fig. 9. It can be seen that a rapid increase of potential with decreasing flow rate, indicating the presence of a substantial volume fraction of gas in the electrode gap, occurs at a higher flow rate in chloride than in nitrate solutions. This shift is consistent with the evolution of a larger gas volume in the first electrolyte.

DISCUSSION

Ohmic Resistance

Since one of the purposes of this study was to define the effect of cathodically generated gas on the electrolyte resistance, the question remains, under which conditions this effect is significant. For the controlled current operation of these experiments, an increase in the ohmic resistance of the electrolyte results in an increase in overall cell voltage. A marked increase in cell voltage, which is observed with decreasing flow rate in 2N KCl (Fig. 10), can be attributed primarily to cathodic phenomena, since anode potentials did not vary by more than 1 to 4 volts for different flow rates. This increase in cell voltage occurs at flow rates which rise with increasing current density and parallels the onset of voltage fluctuations. Although the qualitative influence of gas bubbles on cell voltage is thus strongly indicated, it has not been possible to derive a simple quantitative relation between the gas volume fraction and the cell voltage, which would hold for different current densities. The difficulty may, in part, be due to the fact that the gas was not homogeneously dispersed, neither in the direction normal nor parallel to the electrodes. The bubbles which have been observed to stick to the cathode

surface at flow rates below 400 cm/sec further complicate the situation. Cole and Hopenfeld¹ have also investigated the influence of gas bubbles on cell voltage under ECM conditions. They accounted for the effect of the dispersed gas on the ohmic resistance of the electrolyte by using a relation given by De La Rue and Tobias.¹³ By making certain simplifying assumptions about the two phase region and by adjusting one empirical parameter, they obtained agreement between theoretical and experimental results. The present study suggests, however, that such a simple treatment is not valid for the range of conditions employed here.

Sparking

The formation of continuous gas blankets on vertical wire electrodes in sulfuric acid, at current densities of 6-8 A/cm², has been described by Kellogg.¹⁴ The formation of his gas blanket coincided with a drastic increase in surface temperature and a sharp drop in current. A similar phenomenon also is known to occur in heat transfer under forced convection conditions, where formation of vapor films leads to a sharp reduction in heat flux (burn out, critical heat flux).¹⁵ It was, therefore, of interest to see whether, under ECM conditions, similar gas films are formed and whether they may lead to sparking and electrical breakdown. As long as a sufficiently high flow rate was maintained no such phenomena were observed in the present experiments, even at current densities much higher than those employed by Kellogg. Upon decreasing the flow rate, however, large voltage fluctuations and eventual sparking occurred. These fluctuations, indicated by the broken line in Fig. 10, soon became so large as to impede any measurement upon further reduction of flow rate. A close parallelism between oscillations in cathode potential and cell voltage confirmed the

cathodic origin of the oscillations. The onset of these fluctuations coincided with the appearance of a different type of gas bubble characterized by a large size and odd shape. Picture (a) in Fig. 3 is typical for this situation. It appears that, under these conditions, small individual bubbles are no longer generated and continuous gas pockets may cover a sizeable fraction of the cathode surface. Although an actual sparking event could not be photographed, it is possible that such a breakdown coincides with an instantaneous complete coverage of the cathode. The gas volume fraction, at which uncontrolled fluctuations set in, has been estimated on the basis of current density and flow rate (neglecting gas dissolution) to be approximately 0.4 at 100 and 150 A/cm².

Anode Reactions

Voltage oscillations in constant current electrolysis may also originate at the anode. While a detailed discussion of such phenomena is beyond the scope of the present report, it is interesting to note that the anodic oscillations have been observed under certain conditions with several electrolytes, most notably sodium chlorate. Figs. 12a to c illustrate how the anodic contribution to fluctuations in overall cell voltage U increases in the electrolyte series, chloride, nitrate, chlorate, while the cathodic contribution remains about the same (except for a slight reduction in nitrate, due to the smaller gas volume). Of particular interest are the usually well behaved periodic oscillations which originate at the anode (as indicated by the apparent anode potential e_A in Fig. 12c) in chlorate solution. The frequency of these oscillations depended primarily on current density and was only slightly affected by changes in flow rate. Typical frequencies were 130 and 300 cps at 50 and 100 A/cm², respectively. The voltage fluctuations which originate at the cathode were irregular. Their

frequency was much higher (mostly over 2000 cps) and the amplitude depended strongly on flow rate as well as current density. Periodic phenomena at the anode can be related to the formation of solid films,^{3,16} and Fig. 11 shows indeed how solid dissolution products are being removed from the anode surface, (together with a small amount of gas). Similar, but less pronounced shedding of solid reaction products has been observed in sulfate and nitrate solutions.

The photographic pictures obtained in this study also demonstrate that, under the conditions of a previous investigation of anodic phenomena,³ gas bubbles were usually confined to the vicinity of the cathode. In view of the low solubility of hydrogen gas, it can be concluded that any fraction of the total anodic current possibly used for the oxidation of hydrogen has been negligible. The distribution of gas bubbles in the inter-electrode gap gave no indication of the occurrence of plug flow phenomena, which could drastically affect mass transfer at the anode.

SUMMARY AND CONCLUSIONS

The present study was aimed at providing visual information on cathodic gas evolution during high rate metal dissolution, in order to determine the importance of cathodic phenomena on ohmic electrolyte resistance, anode reactions and sparking. Qualitative rather than quantitative conclusions can be drawn from the results:

1. The size of cathodically generated gas bubbles depends on current density as well as flow rate. At flow rates above 400 cm/sec, only very small bubbles (few microns diameter) were generated and immediately removed by the electrolyte stream.
2. A substantially smaller gas evolution in nitrate than in

chloride solutions has been observed. It indicates the occurrence of cathodic reactions other than hydrogen evolution in the former solution.

3. The influence of cathodically generated gas bubbles on the ohmic cell resistance was very small at flow rates above approximately 1000 cm/sec, for all current densities employed (up to 150 A/cm²). At lower flow rates, this influence can be substantial. Models which are based on a uniformly distributed two phase region and, among other simplifications, neglect the residence time of gas bubbles on the cathode surface, did not predict valid electrolyte resistances.
4. No plug flow phenomena seem to have been induced by the gas evolution under the conditions employed in the present study.
5. The influence of cathodic gas evolution on anodic processes such as mass transfer and current efficiency was usually very small.
6. At insufficient flow rates, strong fluctuations in cell voltages were observed, which coincided with the formation of gas patches at the cathode and which eventually led to electric breakdown. The effect was more pronounced in chloride than in nitrate solutions, in agreement with the fact that less gas was generated in the latter solutions under otherwise identical conditions.
7. In the absence of a theoretical model describing even the most simple single bubble dynamics in a flow field, additional experimental observations are needed to gain even a qualitative

insight into the factors which determine growth, detachment and dispersion of gas bubbles generated at high current densities and electrolyte flow rates in narrow gaps.

ACKNOWLEDGEMENT

This work was conducted under the auspices of the U.S. Atomic Energy Commission.

REFERENCES

1. J. Hopenfeld and R. R. Cole, J. Eng. Ind. 88, 455 (1966).
2. J. Hopenfeld and R. R. Cole, J. Eng. Ind. 91, 755 (1969).
3. D. Landolt, R. H. Muller, and C. W. Tobias, J. Electrochem. Soc. 116, 1384 (1969).
4. G. H. Cook in: Applied Optics and Optical Engineering, R. Kingslake, ed., Vol. 3, p. 118, John Wiley and Sons, New York, 1965.
5. J. Venzcel, Ph.D. Thesis no. 3019, ETH, Zurich, 1961.
6. B. Kabanov and A. Frumkin, Z. Phys. Chem. A 165, 433 (1933).
7. L. S. Tong, Boiling Heat Transfer and Two Phase Flow, p. 138, John Wiley and Sons, New York, N. Y., 1965.
8. J. P. Glas and J. W. Westwater, Int. J. Heat Mass Transfer 7, 1427 (1964).
9. H. Y. Cheh, Ph.D. Thesis, University of California, Berkeley; UCRL-17324 (1967).
10. F. H. H. Valentin, Absorption in Gas Liquid Dispersions, E. F. N. Spon, Ltd., London 1967.
11. International Critical Tables, 3, 272 (1929).
12. F. C. Gunther, Trans. ASME 73, 115 (1961).
13. R. E. De La Rue and C. W. Tobias, J. Electrochem. Soc. 106, 827 (1959).
14. H. H. Kellogg, J. Electrochem. Soc. 97, 133 (1930).
15. S. Levy, in Lecture Series on Boiling and Two Phase Flow for Heat Transfer Engineers, H. A. Johnson, Ed., University of California Extension, Berkeley and Los Angeles, 1965; p. 81.
16. K. Kinoshita, Ph.D. Thesis, University of California, Berkeley, UCRL-19051, Sept. 1969.

FIGURE CAPTIONS

Fig. 1. Optical Arrangement for high speed photography of gas bubbles

- A. Light source (flash)
- B. Flow channel cell
- C. Microscope objective
- D. Telecentric stop
- E. Microscope eyepiece
- F. Beam splitting prism
- G. Magnifier for visual observation
- H. Camera film plane

Fig. 2. Influence of flow rate and cathode orientation on gas evolution in 2 N KCl. Current density 50 A/cm^2 , electrode gap 0.5 mm.

- a. flow rate 100 cm/sec cathode facing down
- b. flow rate 200 cm/sec cathode facing down
- c. flow rate 400 cm/sec cathode facing down
- d. flow rate 100 cm/sec cathode facing up
- e. flow rate 200 cm/sec cathode facing up
- f. flow rate 400 cm/sec cathode facing up

Fig. 3. Influence of flow rate on cathodic gas evolution in 2 N KCl.

Current density 100 A/cm^2 , cathode facing up.

- a. flow rate 400 cm/sec
- b. flow rate 600 cm/sec
- c. flow rate 1000 cm/sec
- d. flow rate 2500 cm/sec

Fig. 4. Influence of current density on cathodic gas evolution in 2 N KCl.

Flow rate 100 cm/sec, cathode facing down.

Fig. 4., cont.

- a. Current density = 5 A/cm^2
- b. Current density = 20 A/cm^2
- c. Current density = 50 A/cm^2

Fig. 5. Distribution of cathodic gas bubble diameters in 2 N KCl. 50 A/cm^2 , 100, 200 and 400 cm/sec. Total number of bubbles measured 31, 43 and 50 respectively, for cathode facing up (---) and 27, 32, 60 respectively, for cathode facing down (—). (Counts incomplete in range 0-25 μ , due to lack of resolution below 20 μ).

Fig. 6. Distribution of cathodic gas bubble diameters in 2 N KCl. Flow rate 100 cm/sec, current density 5, 20 and 50 A/cm^2 . Total number of bubbles measured 47, 47 and 31, respectively for cathode facing up (---) and 37, 42 and 27, respectively, for cathode facing down (—). (Counts incomplete in range 0-25 μ , due to lack of resolution below 20 μ).

Fig. 7. Cathodic gas evolution at 100 A/cm^2 in 2 N KNO_3 and 2 N KCl, cathode facing down.

- a. KCl, flow rate 400 cm/sec
- b. KCl, flow rate 800 cm/sec
- c. KNO_3 , flow rate 400 cm/sec
- d. KNO_3 , flow rate 800 cm/sec

Fig. 8. Apparent volume fraction of interelectrode gap occupied by two phase region (gas-electrolyte mixture).

- 2 N KCl, 400 cm/sec
- 2 N KCl, 800 cm/sec

Δ 2 N KNO₃, 400 cm/sec

▲ 2 N KNO₃, 800 cm/sec

Fig. 9 Effect of gas evolution in different electrolytes on apparent cathode potentials, measured vs. sat. calomel with capillary upstream from the electrode. Current density 100 A/cm², cathode facing up.

Δ 2 N KCl

□ 2 N KNO₃

--- amplitude range of voltage fluctuations

Fig. 10. Effect of gas evolution in 2 N KCl at different current densities on cell voltage.

● cathode facing down

○ cathode facing up

--- amplitude range of voltage fluctuations

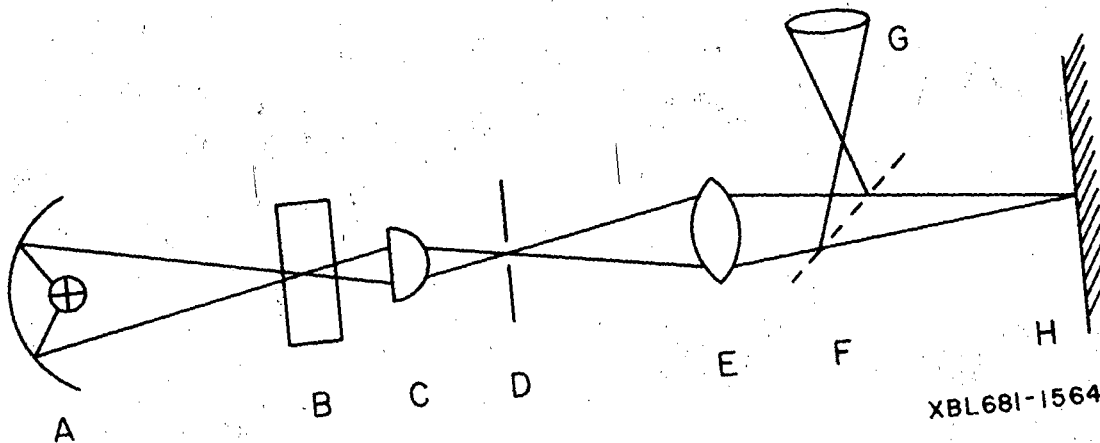
Fig. 11. Anodic dissolution products generated in 2 N NaClO₃ at 50 A/cm² and 100 cm/sec. Cathode facing up.

Fig. 12. Typical recorder traces of cell voltage U, current I, apparent anode potential e_A and apparent cathode potential e_C. 50 A/cm², 400 cm/sec.

a. 2 N KCl

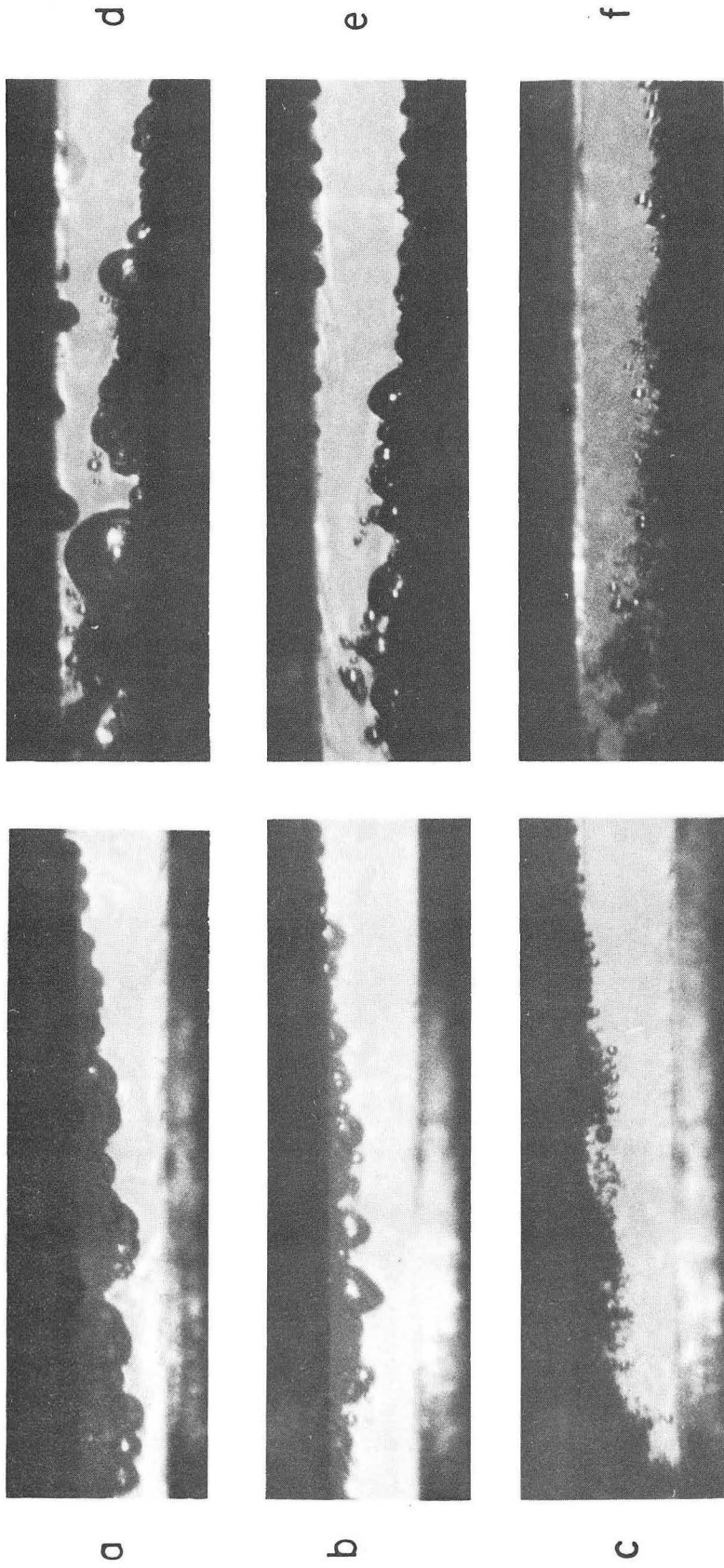
b. 2 N KNO₃

c. 2 N Na ClO₃



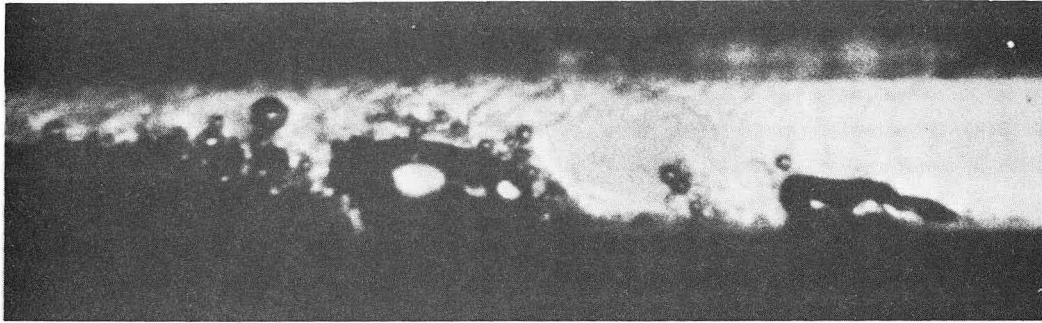
XBL681-1564

Fig. 1

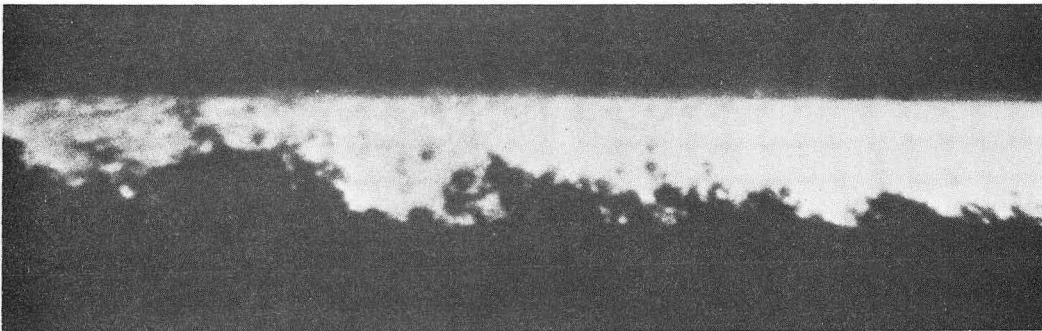


XBB 699-5795

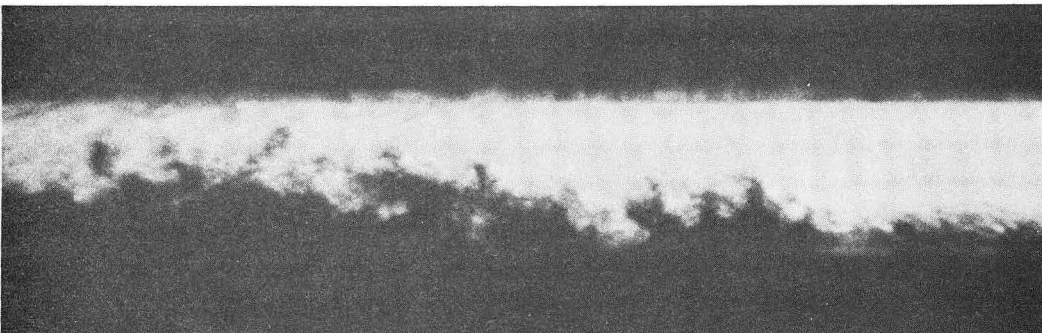
Fig. 2



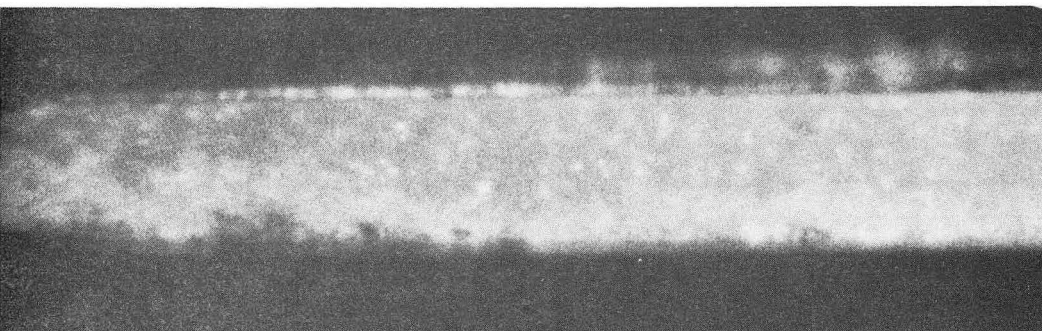
a



b



c



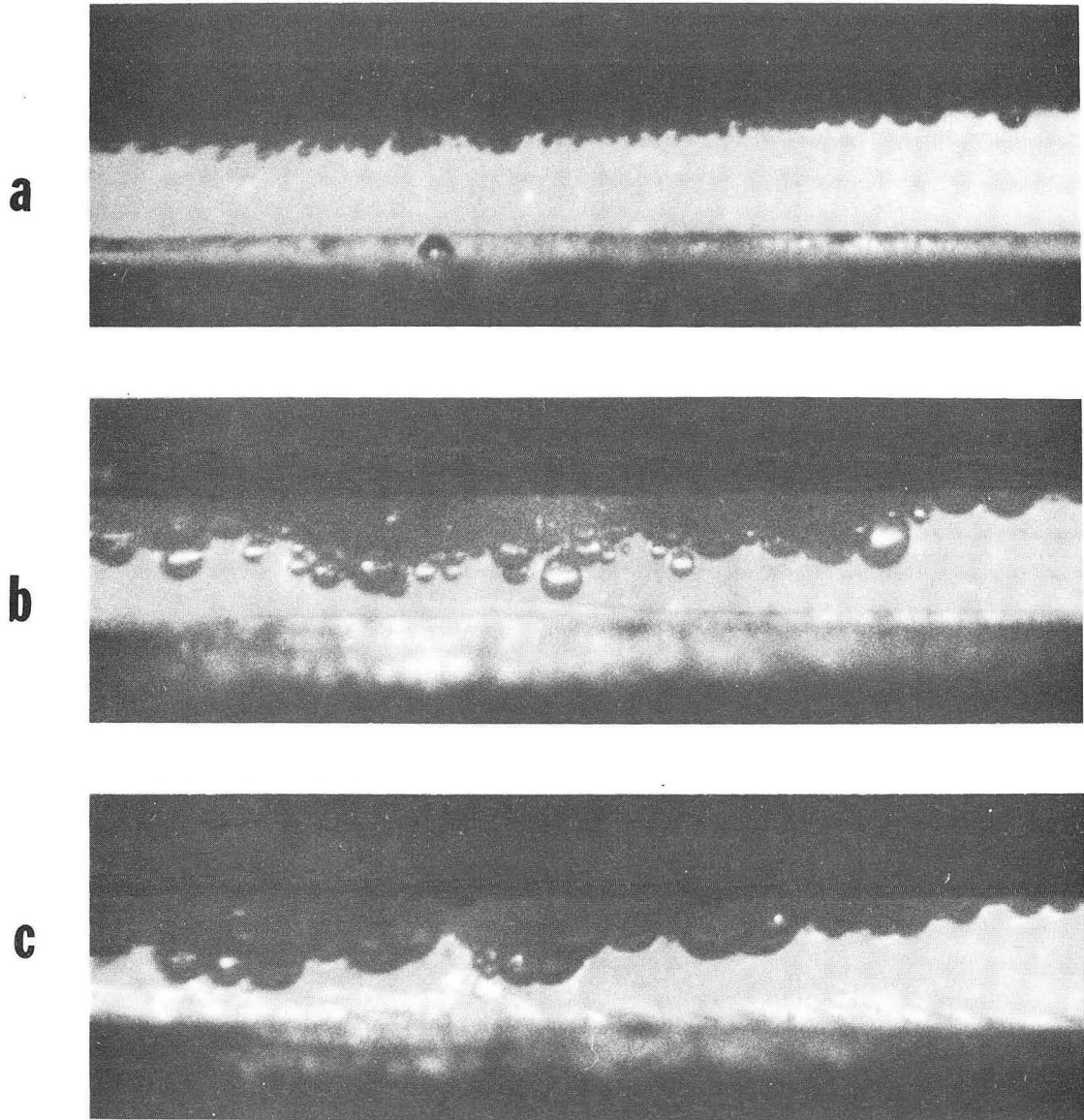
d



Flow

XBB 699-5796

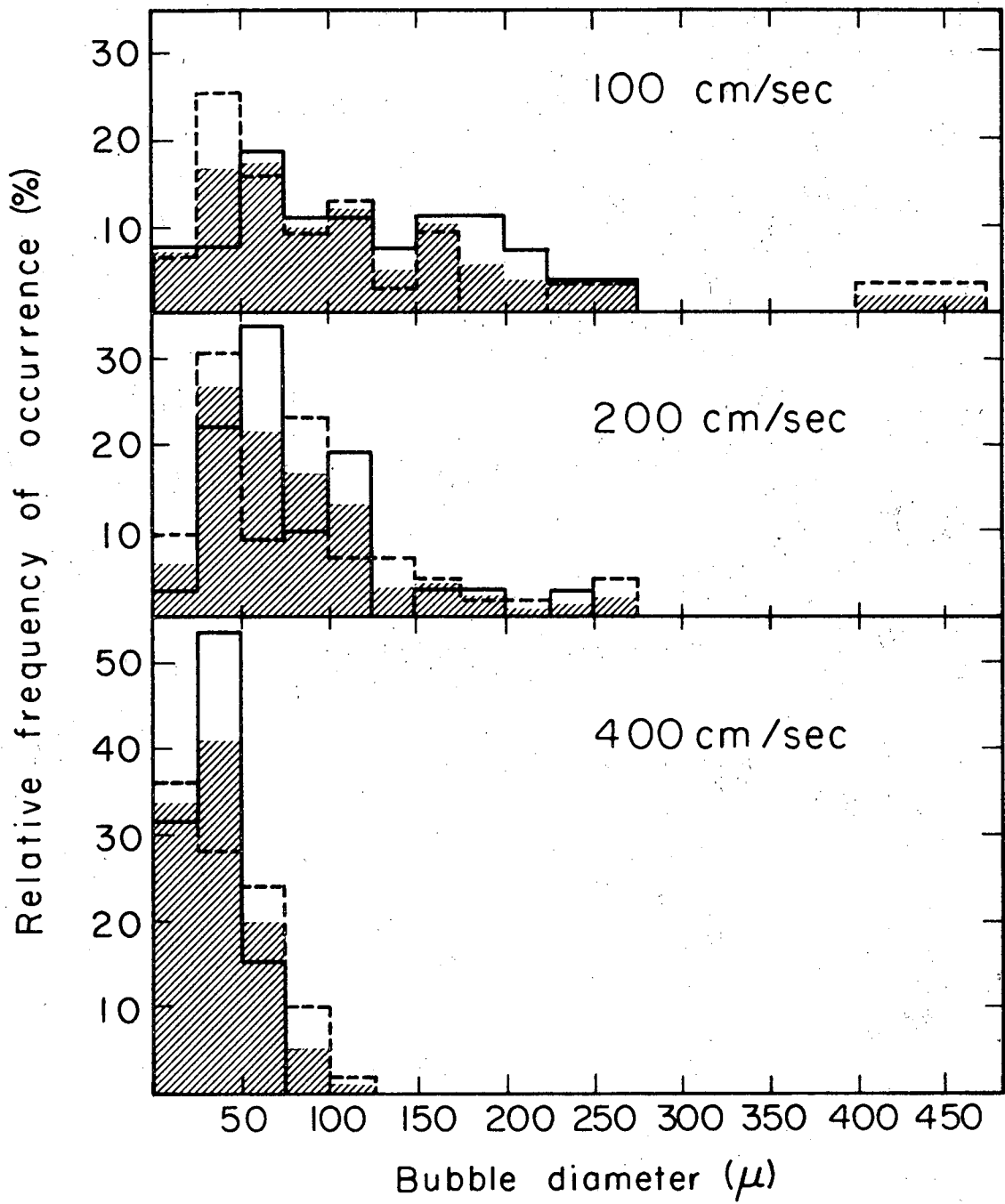
Fig. 3



← Flow

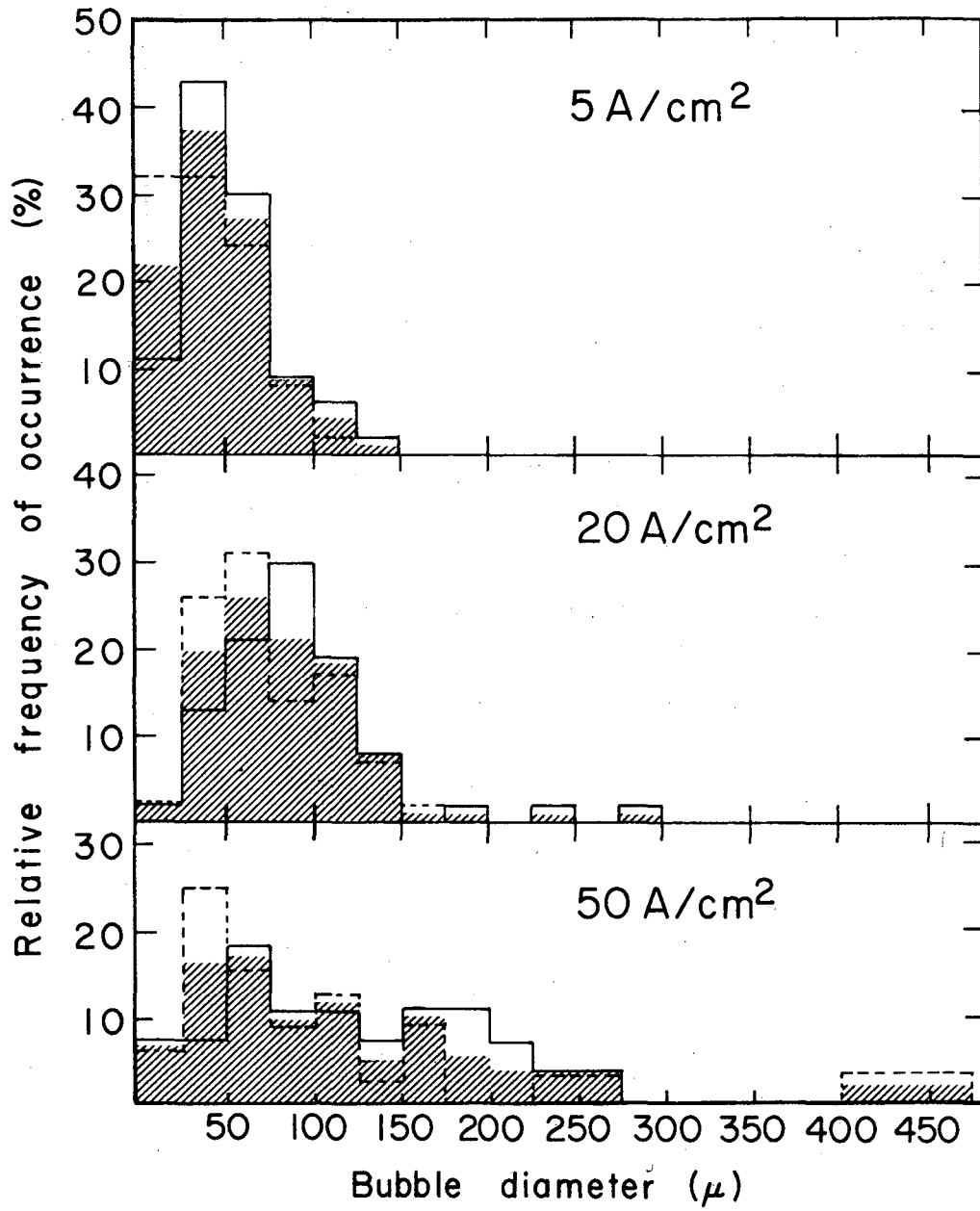
XBB 7912-7685

Fig. 4



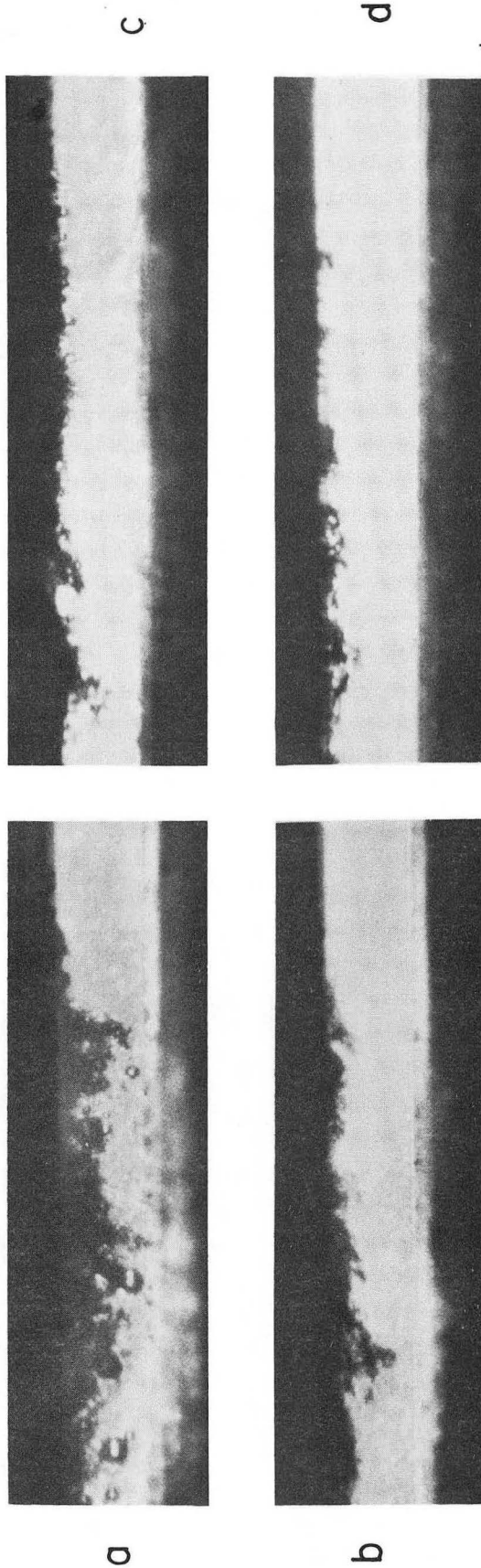
XBL698-3569

Fig. 5



XBL6911 - 6205

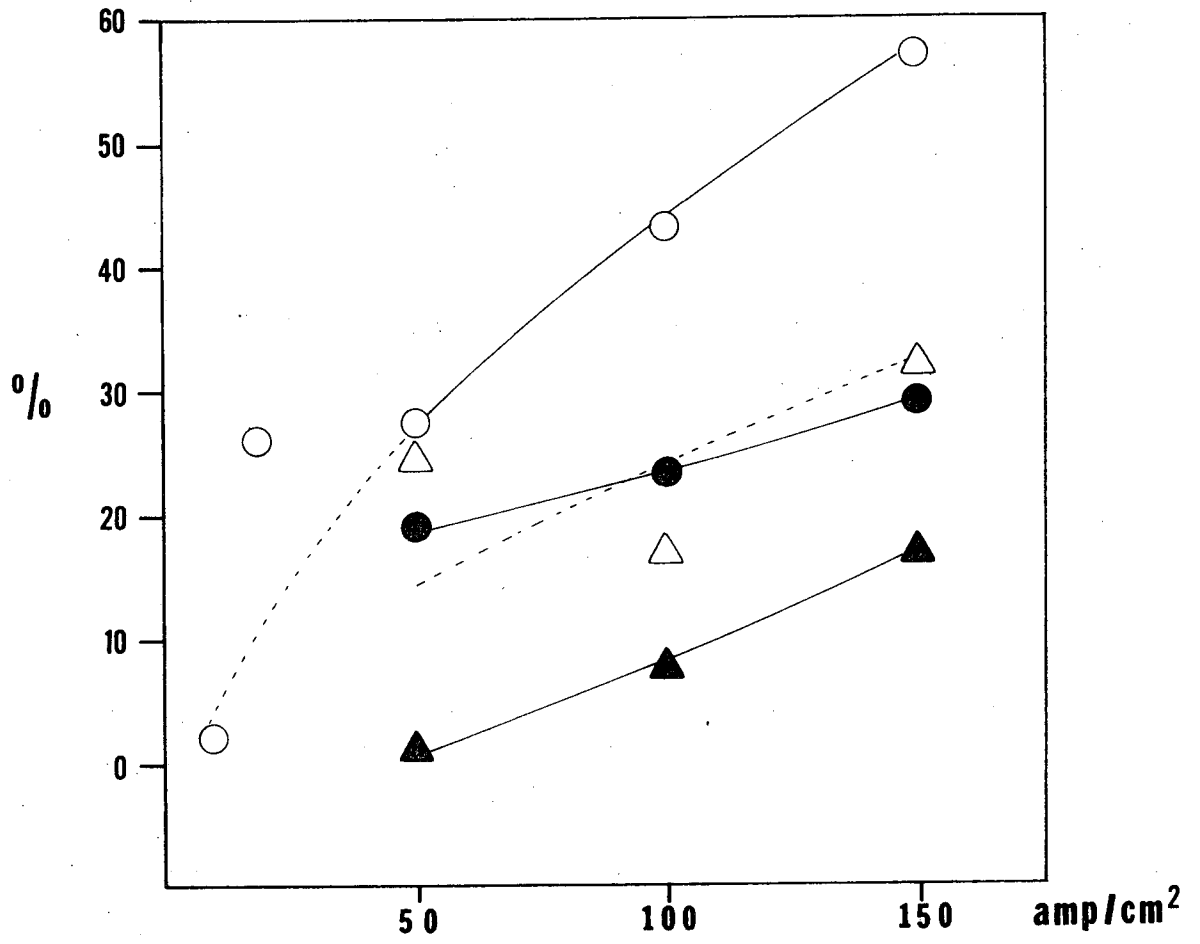
Fig. 6



← FLOW

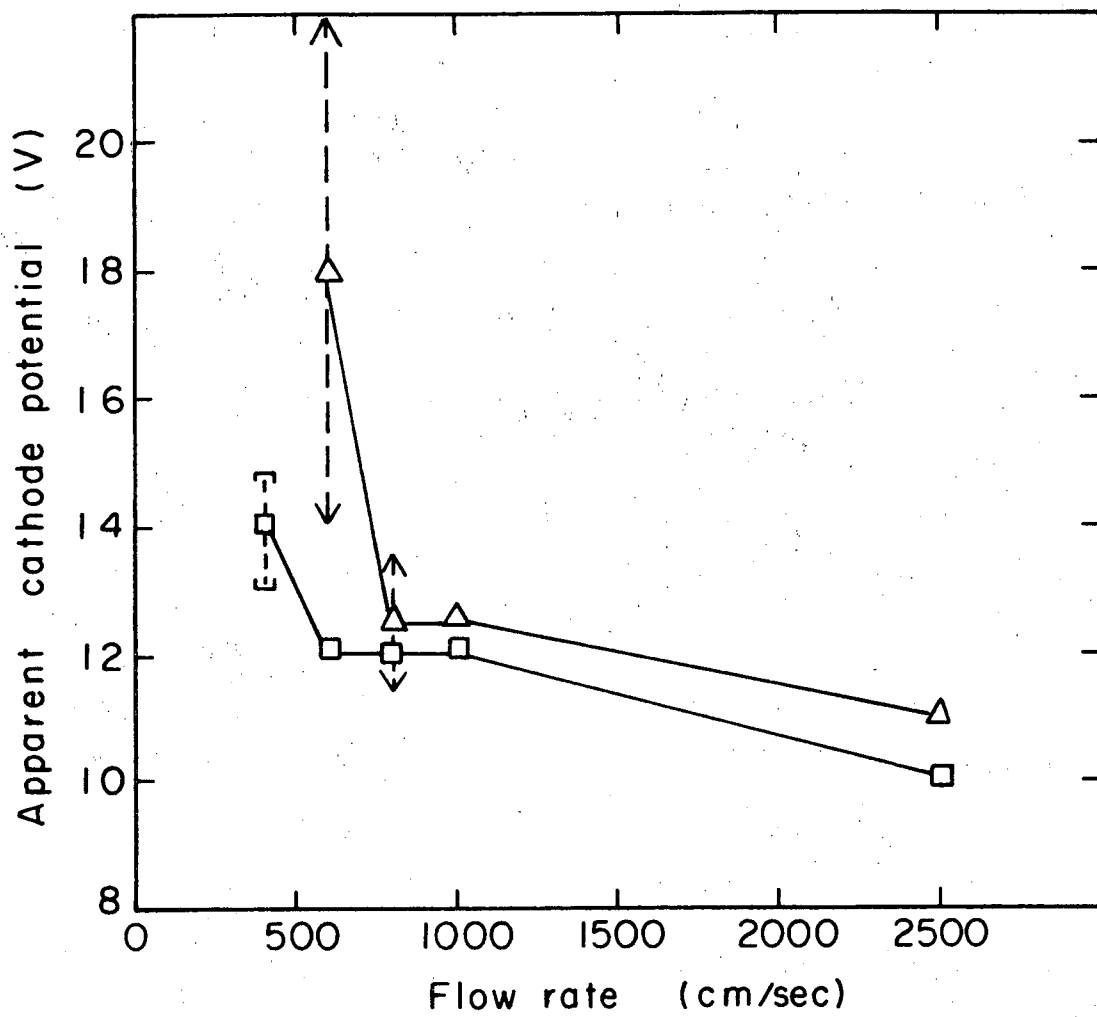
XBB 699-5797

Fig. 7



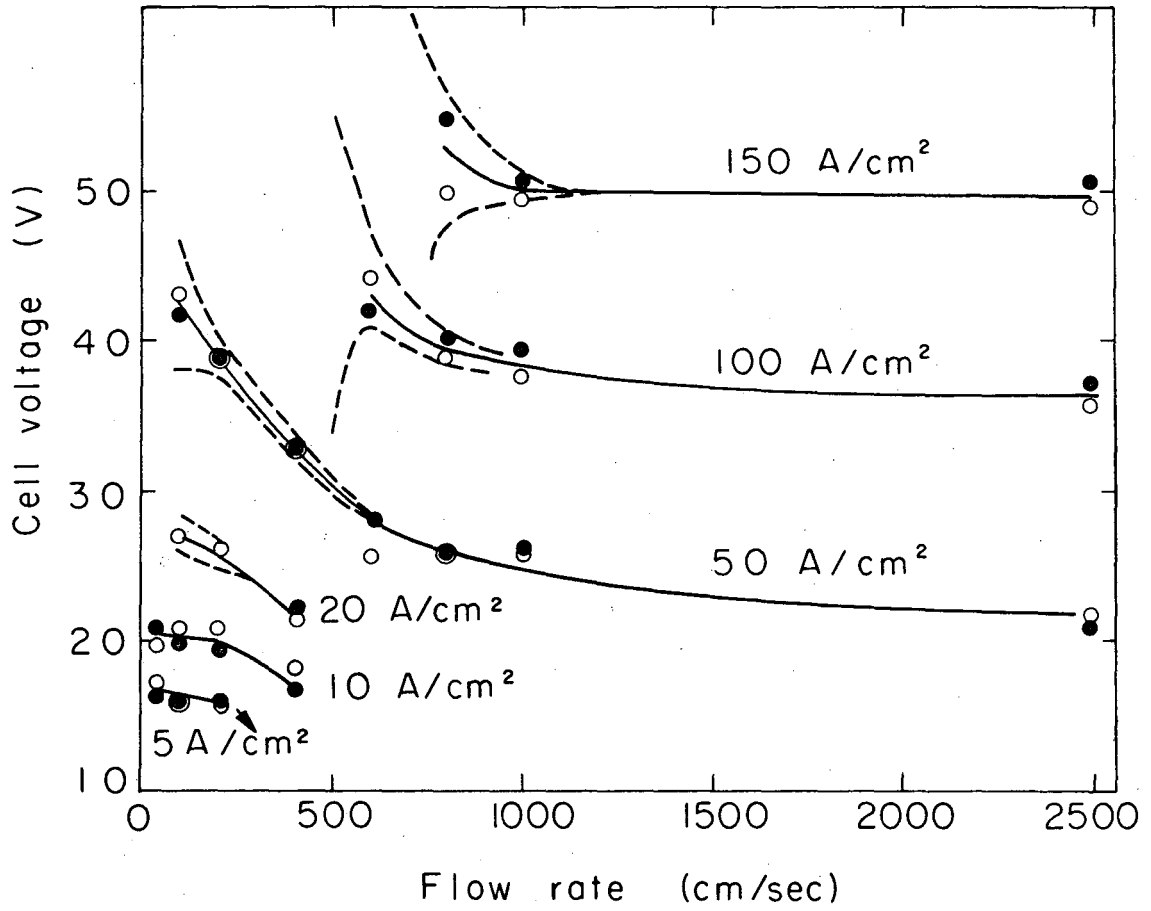
XBL 6911-6512

Fig. 8



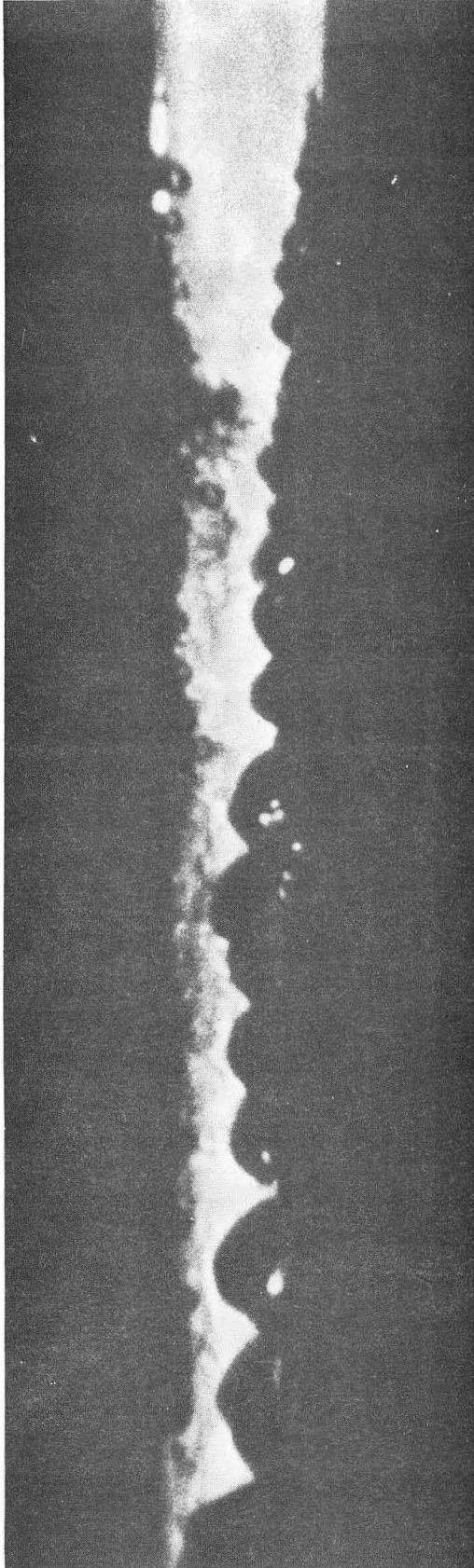
XBL 698-3570-A

Fig. 9



XBL 698 - 3571

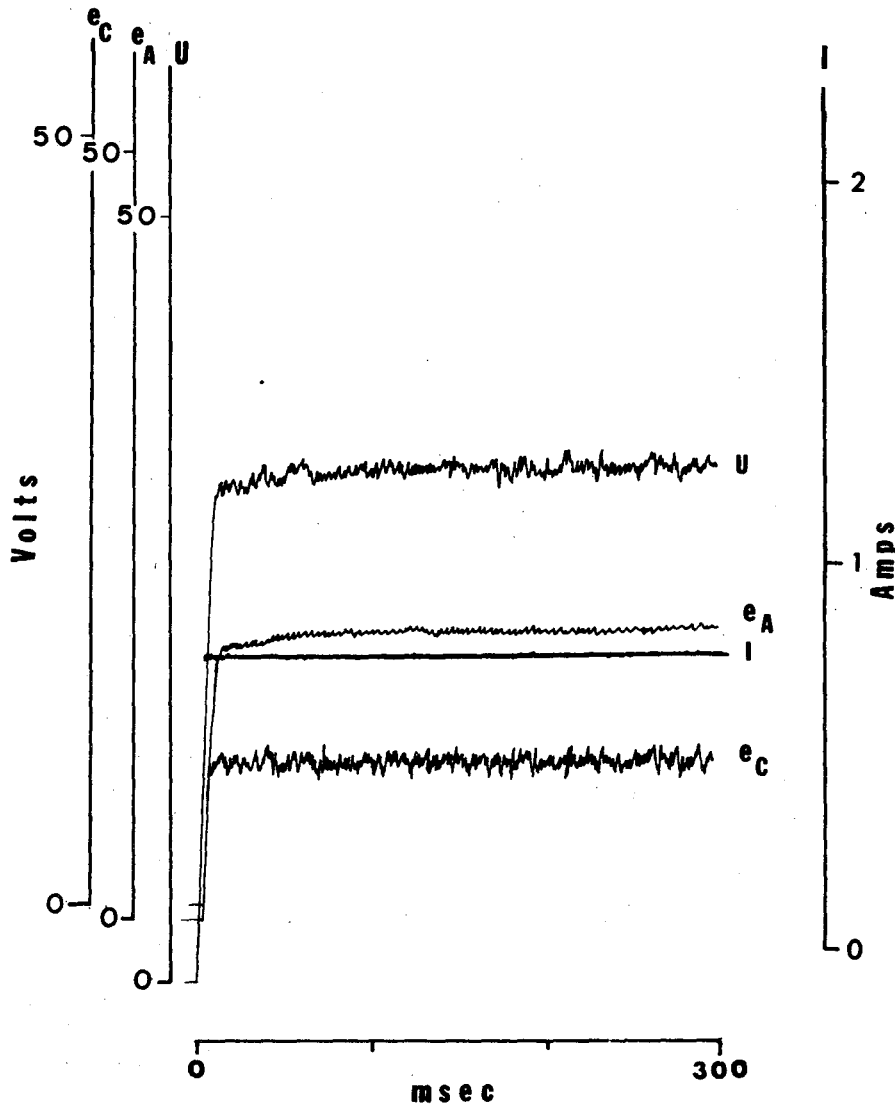
Fig. 10



← FLOW

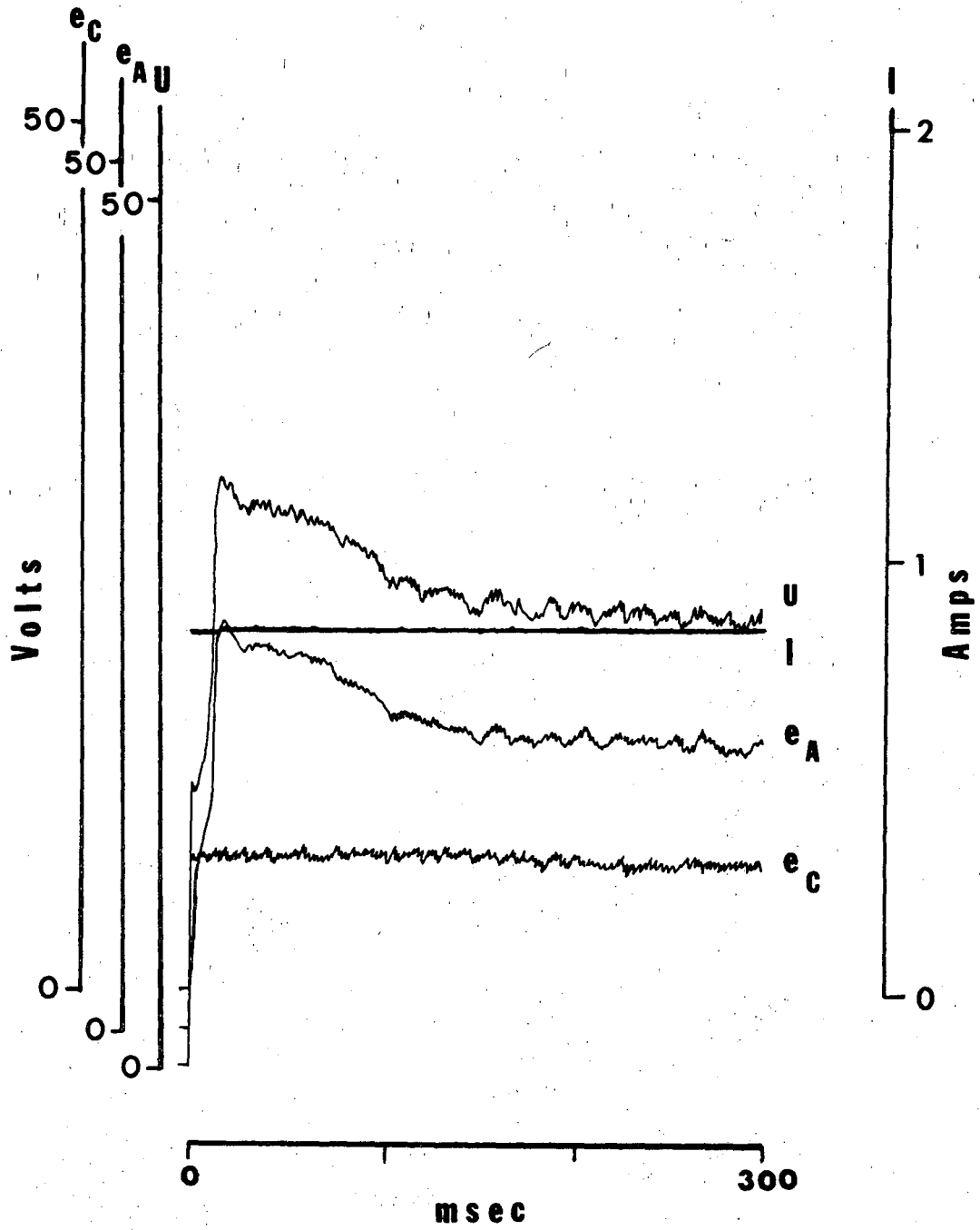
XBB 699-5798

Fig. 11



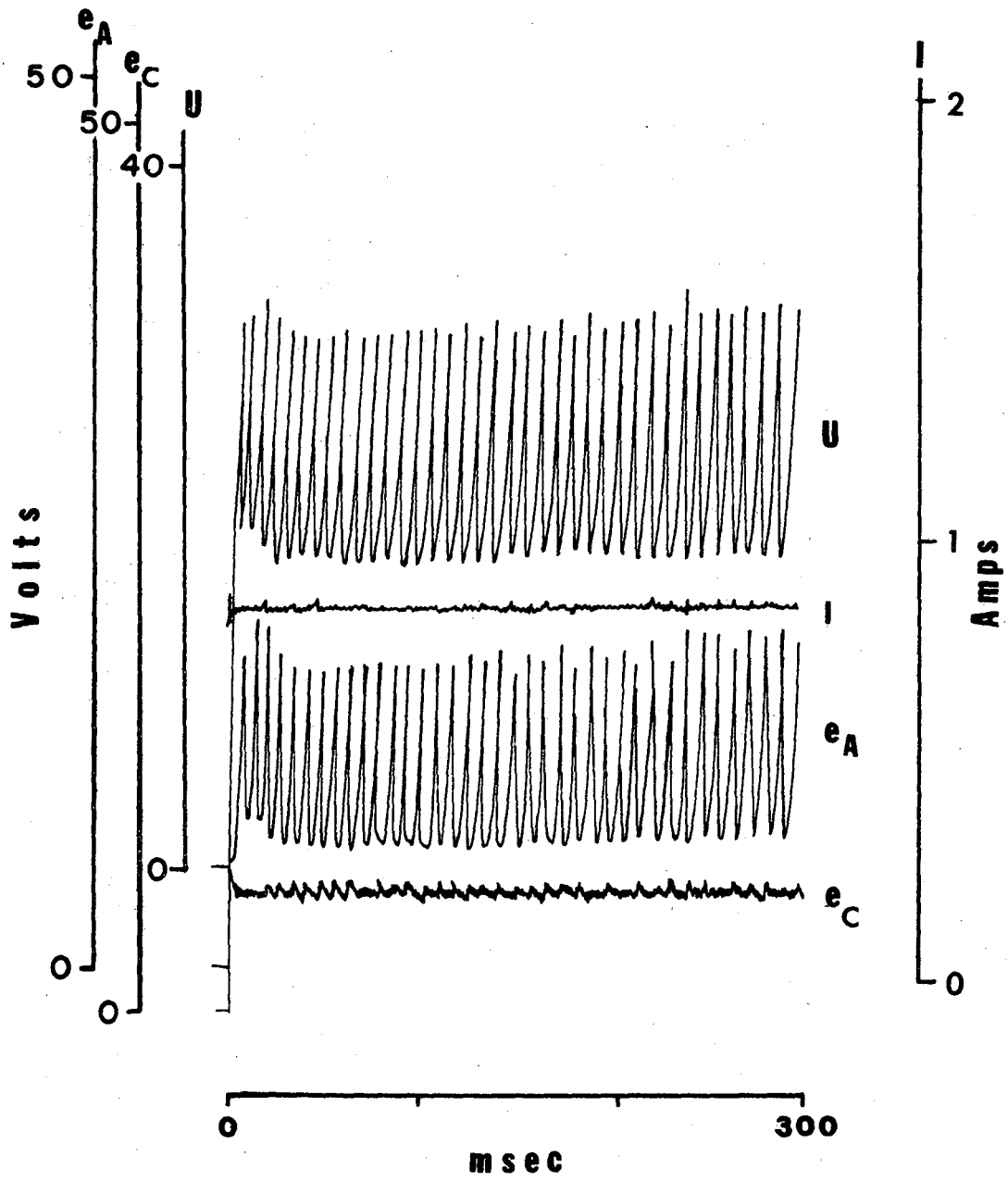
XBL698 - 3565

Fig. 12a



XBL698-3566

Fig. 12b



XBL698-3567

Fig. 12c

LEGAL NOTICE

This report was prepared as an account of Government sponsored work. Neither the United States, nor the Commission, nor any person acting on behalf of the Commission:

- A. Makes any warranty or representation, expressed or implied, with respect to the accuracy, completeness, or usefulness of the information contained in this report, or that the use of any information, apparatus, method, or process disclosed in this report may not infringe privately owned rights; or*
- B. Assumes any liabilities with respect to the use of, or for damages resulting from the use of any information, apparatus, method, or process disclosed in this report.*

As used in the above, "person acting on behalf of the Commission" includes any employee or contractor of the Commission, or employee of such contractor, to the extent that such employee or contractor of the Commission, or employee of such contractor prepares, disseminates, or provides access to, any information pursuant to his employment or contract with the Commission, or his employment with such contractor.

TECHNICAL INFORMATION DIVISION
LAWRENCE RADIATION LABORATORY
UNIVERSITY OF CALIFORNIA
BERKELEY, CALIFORNIA 94720